

A QUANTUM OPTICS LAB USING PHOTON PAIRS

by

David Gorski

A Thesis Submitted to the Faculty of

The Wilkes Honors College

in Partial Fulfillment of the Requirements for the Degree of

Bachelor of Science in Liberal Arts and Sciences

with a Concentration in Physics

Wilkes Honors College of

Florida Atlantic University

Jupiter, Florida

May 2019

A QUANTUM OPTICS LAB USING PHOTON PAIRS

by

David Gorski

This thesis was prepared under the direction of the candidate's thesis advisor, Dr. Yaouen Fily, and has been approved by the members of his supervisory committee. It was submitted to the faculty of the Harriet L. Wilkes Honors College and was accepted in partial fulfillment of the requirements for the degree of Bachelor of Science in Liberal Arts and Sciences.

SUPERVISORY COMMITTEE:

Dr. Yaouen Fily

Dr. Chitra Chandrasekhar

Dean Ellen Goldey, Harriet L. Wilkes Honors College

Date

Acknowledgements

I could not have completed this thesis, nor my degree, without the guidance, encouragement, and kindness of Dr. Yaouen Fily.

The advice provided by Dr. Chitra Chandrasekhar was invaluable in drafting this thesis.

This entire lab was conducted at SUNY Geneseo, under the supervision of Dr. George Marcus. His mentorship and guidance made the completion of this lab possible at all.

The kindness and support of my family and friends cannot be overstated. I owe any accomplishments to all the wonderful people in my life. I especially want to thank my mom and brother for being so supportive throughout my college years.

Abstract

Author: David Gorski
Title: A Quantum Optics Lab using Photon Pairs
Institution: Harriet L. Wilkes Honors College, Florida Atlantic University
Thesis Advisor: Dr. Yaouen Fily
Degree: Bachelor of Science in Liberal Arts and Sciences
Concentration: Physics
Year: 2019

Quantum Mechanics is a difficult and unintuitive theory for undergraduate students to understand, but a lab in which students directly observe quantum phenomena will help students understand the theory. Utilizing a relatively simple setup it is possible to reproduce a large number of foundational single-photon experiments. The lab employs correlated photon pairs to simulate single photons. With this setup students are able to verify first-hand the existence of photons through the Hanbury Brown-Twiss experiment and the wave-like behavior of light through single-photon interference in a Mach-Zehnder interferometer. I have also created informative visualizations that aid in the understanding of the counter-intuitive nature of quantum mechanics and the laboratory setup. More experiments could be added to this curriculum with relative ease highlighting other aspects of quantum mechanics.

To Babcia

Contents

Abstract	iv
1 Introduction	1
2 Single Photon Down Conversion	3
2.1 Experimental Setup	4
2.2 Explanatory visualization of Parametric Down Conversion	6
2.3 Testing Time Lag	6
3 Hanbury Brown-Twiss	8
3.1 Experimental Setup	9
3.2 Explanatory visualization of Hanbury Brown-Twiss	9
3.3 Data Interpretation and Analysis	10
4 Single Photon Interference	12
4.1 Experimental Setup	12
4.2 Explanatory visualization of Single Photon Interference	13
4.3 Single Detector Results	13
4.4 Dual Detector Results	16
5 Possible Improvements and Extensions	17
A Equipment	18
B Mach Zehnder Interferometer Alignment	23
C Procedures	24
C.1 Initial Setup	24
C.2 Parametric Down Conversion	25
C.3 Hanbury Brown-Twiss	25
C.4 Single Photon Down Conversion	26

List of Tables

1	Detection and coincidence counts with varied time lag	7
2	Expected and Observed count/coincidence rates for the Hanbury Brown-Twiss experiment	10

List of Figures

1	A coincidence between two detectors	3
2	Schematic representation of parametric down conversion	5
3	Visualization of Parametric Down Conversion	6
4	Schematic representation of the Hanbury Brown-Twiss experiment	9
5	Visualization of Hanbury Brown-Twiss	9
6	Schematic representation of the Single Photon Interference experiment	12
7	Visualization of Single Photon Interference	13
8	Data from detector A placed at the end of a single arm of the MZI	13
9	Data from both detectors of the MZI	16
10	HeNe and Blue laser paths	18
11	Beam-splitter paths	18
12	Mach-Zehnder Interferometer	19
13	Graph of blue laser polarization	20
14	FPGA and converter box	20
15	Labview data collection	21
16	HeNe interference pattern	23
17	MZI alignment through white light interference	23

1 Introduction

The discovery of the quantization of light and subsequent theory of quantum mechanics were pivotal in the development of modern physics. It is imperative to help students master quantum mechanics so that they can get a more accurate picture of our physical reality. Newtonian mechanics has long been taught to students and an intuitive mental model of these mechanics can be developed by students with relative ease. In contrast, quantum mechanics presents a counter-intuitive picture of our physical world that we hardly encounter in everyday life. Light seems to behave as a wave in our everyday life; however, we learn through quantum mechanical theory that light can be understood as coming in discrete packets. Although students may be exposed to this idea in their coursework, it is often difficult for students to connect this to our physical reality. Undergraduate laboratory courses play an important role in helping students solidify their understanding of the material by providing a hands-on experience that enables students to build an intuitive model. The basis of modern physics requires the same degree of laboratory exposure to enable the next generation of students to build a deep understanding. In order to explore these quantum phenomena in an undergraduate setting, I have streamlined a series of quantum optics experiments in order to showcase the quantum nature of our world first-hand. This work builds upon a body of existing work, especially the work of Dr. Enrique (Kiko) Galvez. By highlighting light quantization, I hope to excite students to explore modern physics more deeply and provide a lasting understanding of the basics of quantum mechanics that would not be possible in a classroom environment. The equipment we have used in constructing this undergraduate lab is all available off the shelf from a variety of manufacturers for relatively affordable prices, and as the production of these pieces is streamlined the prices will drop further. The most expensive component used in our setup is an optical workbench. All of the experiments sit on this workbench, so this workbench is a vital part of the experimental setup; however, the lab employs several cost-cutting methodologies.

This paper is broken down into three major experiments. Section 2 discusses the appropriate setup of the lab equipment and the approximation of single photons through the use of

correlated photon pairs. Section 3 is a recreation of the foundational Hanbury Brown-Twiss experiment, proving the existence of photons. Finally, Section 4 concludes the lab with an analysis of single photon interference utilizing a Mach-Zehnder Interferometer. Following these experiments Section 5 contains a small discussion of possible extensions to this lab. The Appendices A-C contain detailed information about the specific implementation of the lab equipment.

2 Single Photon Down Conversion

It is very difficult and expensive to produce single photons reliably. Thus, this lab has followed the lead of others in utilizing photon pairs to simulate single photons. By producing a pair of correlated photons, we can be sure that they are traveling in a known direction and originate from the same location at the same time. Because these photons are temporally correlated, if two photons arrive at two equally spaced detectors at the exact same time, it is certain that they are from the same pair. However, our environment has stray photons which will occasionally be detected by our single photon detectors. A single dual detection event (both detectors detecting photons at the same time, possibly indicating a photon pair) is therefore not enough to ensure that we are detecting the photons from our photon pair, but by using a whole stream of these photon pairs it is possible to identify that the system as a whole is detecting individual photons from our pair instead of any stray photons from the environment.

Whenever a single photon arrives at our detectors, an electric pulse of finite length, τ is generated. When the pulses from the two detectors overlap, the photon detection events have overlapped. This simultaneous dual detection is labeled a 'coincidence' between two detectors. Our photon pairs should register as coincidences while the optical path length to each of our detectors is equal (or more precisely, the difference is less than τc).

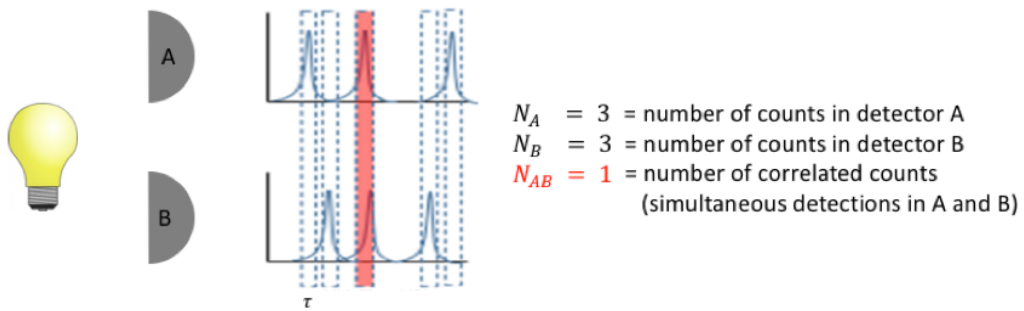


Figure 1: A coincidence between two detectors. Voltage outputs graphs are shown for detectors A and B. Each blue box is of width τ seconds. The red box is the only τ time window in which the outputs overlapped, this overlap is a coincidence. [4]

Since there are stray photons in the environment one can expect uncorrelated photons to occasionally overlap and thus introduce accidental coincidence counts. We calculate our expected amount of accidental overlap between random photons arriving as

$$N_{accidental} \propto \tau N_A N_B \quad (1)$$

where N_A is detector A's counts, N_B is detector B's counts, and τ is the pulse width of our detectors. Our pulse width represents the temporal width of our counts: a count occurring at time t will have a width of $t + \tau$, another pulse starting anywhere in this window of time will be counted as a coincidence; thus, our accidental rate is proportional to the pulse width.

It is useful to introduce an anti-correlation parameter α :

$$\alpha = N_{AB}/\tau N_A N_B \quad (2)$$

Here, N_{AB} is the total coincidence count and the denominator is the predicted accidental count, Eq. (1). This single parameter is a measure of the correlation of the system which can be used instead of keeping track of all other parameters. In the case where there are an insufficient number of correlated photons, the number of coincidences in the system is below or equal to the accidentally expected number, therefore $\alpha \leq 1$. Whereas a value of $\alpha > 1$ corresponds to a correlated system where it is certain there are correlated photons being detected. By referencing this single value, one can identify if a system is measuring correlated photons. [5]

2.1 Experimental Setup

In order to show the quantum mechanical properties of light we must have a reliable source of single photons. This lab employs a non-linear crystal, in our case Beta Barium Borate (BBO) although alternatives such as Lithium Triborate (LBO) will also work, in order to create correlated photon pairs. To confirm whether our laboratory system is producing correlated photon pairs it is necessary to measure an $\alpha > 1$. Establishing a correlated

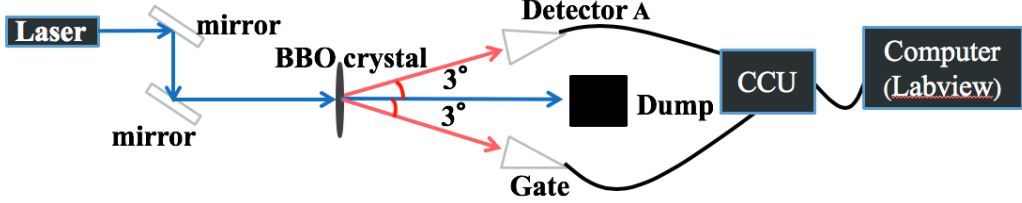


Figure 2: Schematic representation of parametric down conversion

system is the first step in every experiment throughout this lab.

Blue laser light of wavelength 405nm is sent through a non-linear BBO crystal and is partially converted to correlated infrared light by the crystal, but the majority of the blue beam passes through the crystal and is sent to a beam dump so as not to interfere with the rest of the experiment. The BBO crystal creates correlated photon pairs at twice the original wavelength: 810nm. The BBO crystal is cut so that photon pairs exit in a 3° cone. By placing the detectors along this cone, we can observe the photon pairs that exit the cone parallel to our table's surface. This simple setup will confirm the lab setup and equipment is functional.

The detectors output a voltage spike to the high-speed electronics when they receive a photon. Using a pulse width of this voltage spike of just 8ns we are able measure an $\alpha > 1$ (the first data column of Table 1) confirming that our detectors are seeing correlated photons coming from the BBO crystal:

$$\alpha = \frac{794}{8 \times 10^{-9} * 9597 * 81066} = 127.6 \quad (3)$$

Note, in this case the gate signal (81066) is much higher than the signal to detector A (9597). This is due to misalignment in our setup, but a certain amount of misalignment is expected. As long as our system has an $\alpha > 1$ we can be certain we are detecting the single photon pair.

2.2 Explanatory visualization of Parametric Down Conversion

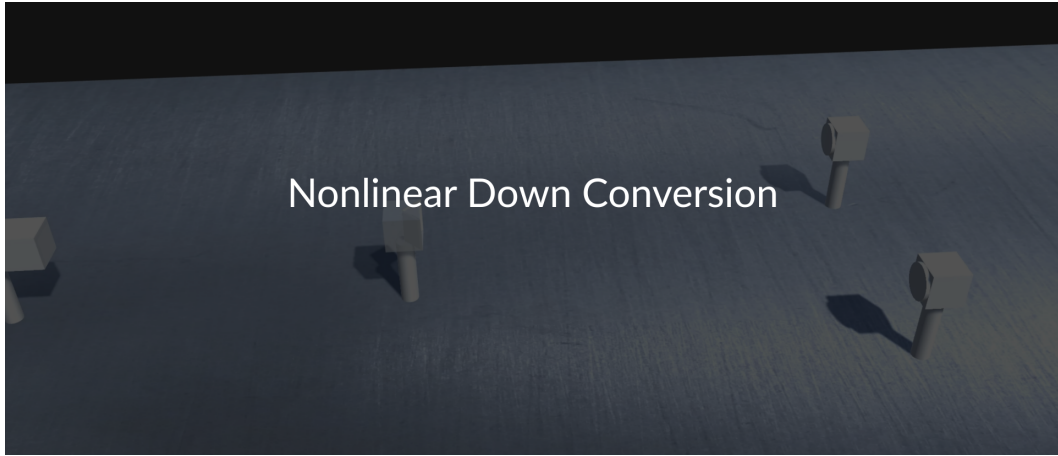


Figure 3: Link to a visualization of the down conversion experiment.

<https://youtu.be/5Iv6dJD4q4A>

2.3 Testing Time Lag

It is also necessary to check the functioning of the electronics used in this setup. By placing a longer cable between our detectors and electronics we are able to introduce systematic delay: it now takes a few nanoseconds longer for our detector's pulse to arrive to our electronics. The highspeed electronics used are able to shorten the pulse width from our detector's initial pulse width of 42ns down to 8ns; because of this short pulse width even just a few nanoseconds of delay introduced by a slightly longer cable between one of our detectors is enough to eliminate the coincidences between the two detectors.

To further check the functioning of our experiment we increase the pulse width (the high-speed electronics enable this). If the increase to the pulse width is larger than the delay introduced by the cable, there should again be coincidences as the pulses now are wide enough to overlap even with the delay. This will confirm that our pulse shortening is working as intended.

	Equal Size Cables (8ns)	Unequal Size Cables (8ns)	Unequal Size Cables (18ns)
A	9597	9353	9382
Gate	81066	78139	78266
A+Gate	794	6	606
α	127	1.03	45.8

Table 1: Detection and coincidence counts with varied time lag. The A row represents the count rate for the A detector. The Gate row represents the count rate for the second detector. The A+Gate row represents the coincidences between detections between A and Gate. The anti-correlation factor, α , is also shown for each setup. Counts are summed over a 25s period to obtain the rates.

Table 1 displays two trials at a $\tau = 8\text{ns}$, where one has equally long cables from each detector to the high-speed electronics setup and the other trial has a longer cable placed from detector A to the high-speed electronics. The coincidences between the two detectors all but disappear when this longer cable is introduced, this makes sense as our pulse from detector A is slightly delayed on the way to the electronics. Note that even though $\alpha > 1$ in our second trial, it is so close to $\alpha = 1$ as to be considered uncorrelated. By adjusting the pulse width to $\tau = 18\text{ns}$ we are able to recover most of the coincidences indicating that we have successfully broadened the pulse width so that the delay introduced by the cable is no longer relevant. This step further confirms the proper functioning of the high-speed electronics. Detailed instructions on procedures to achieve this proper setup can be found in Appendix C.

3 Hanbury Brown-Twiss

In order to highlight quantization in quantum mechanics, and to prove the existence of photons, this lab employs the Hanbury Brown-Twiss experiment (HBT). Classically, light is understood strictly as a wave phenomenon, and so a light ray incident on a half-silvered mirror (a beam-splitter) will be split. In our lab we use a beam-splitter with half transmission and reflection rates; thus, half the intensity of our light should come through each path. We probe this behavior by sending infrared light from the BBO crystal through the beam-splitter. Through the strictly classical picture, our infrared light should be split in intensity and find its way to down both paths. We will test this experimentally by placing detectors at the end of both paths of the beam-splitter.

If photons exist, light is not simply split evenly in intensity, but instead a photon is either transmitted or reflected. A single photon passing through the beam-splitter cannot travel through both paths to detectors A and B simultaneously. Therefore, we expect an $\alpha > 1$ for both detectors with regard to the flag detector and an $\alpha < 1$ between detectors A and B. This would mean that the stream of correlated photons is being split and a photon from the correlated pair is arriving at either detector A or B, but never both. This makes intuitive sense if light is understood as strictly a particle phenomenon.

3.1 Experimental Setup

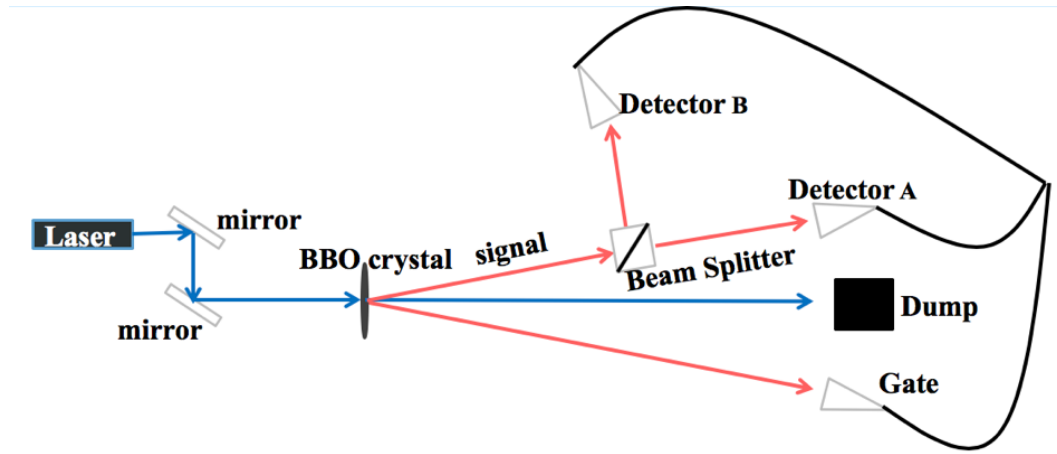


Figure 4: Schematic representation of the Hanbury Brown-Twiss experiment

Note the similarity of this setup to the previous experiment. The change in experimental setup simply involves placing a beam-splitter in one of the paths of the photon pair and placing a detector in the new path of reflected light.

3.2 Explanatory visualization of Hanbury Brown-Twiss

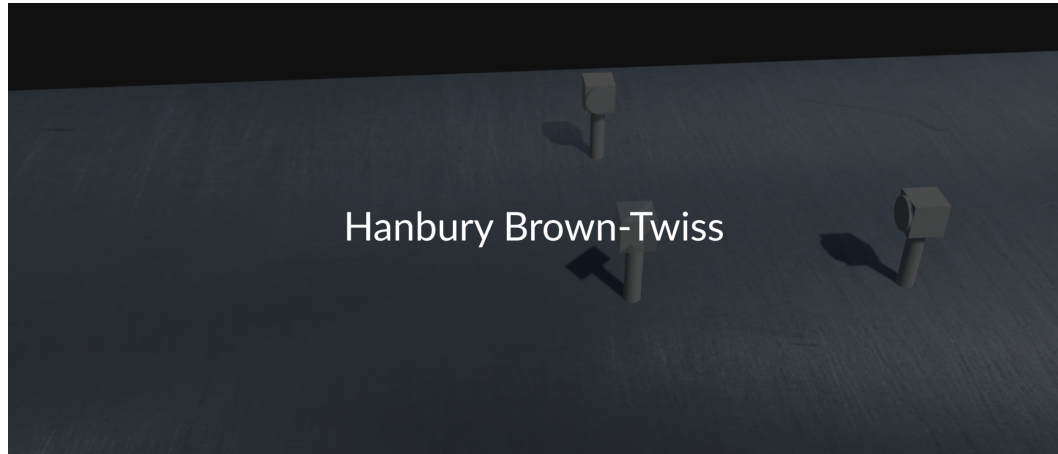


Figure 5: Link to a visualization of the Hanbury Brown-Twiss experiment.
<https://youtu.be/-yTW3Zmfqks>

3.3 Data Interpretation and Analysis

	A	B	G	AB	AG	BG	ABG
Expected	36987 ±83	36987 ±83	69652 ±118	7.20 ±1.2	1753 ±19	1753 ±19	1.70 ±0.58
Observed	20358 ±64	14558 ±54	69652 ±118	2.70 ±0.47	1437 ±17	1417 ±17	0.37 ±0.28

Table 2: Expected and Observed count/coincidence rates for the Hanbury Brown-Twiss experiment. Counts are the average of 5 runs each summed over a 25s period to obtain the rates.

In Table 2, based on the count rates without the beam-splitter present, expected count rates were calculated for a 50/50 beam-splitter. The uncertainties are measured by a counting error which is calculated as half the value of the average count rate.

Before placing our beam-splitter we are able to generate expected results for the existence of photons in our experiment. The counts for A and B are each half of the counts at A before the beam-splitter is placed. The Gate counts remain the same. The coincidences between detector A and Gate detector (AG) and detector B and Gate detector (BG) are each half of the coincidences in our system before the beam-splitter. The coincidences between detectors A, B, and Gate (AB and ABG) is only equal to the accidental rate. Our generated data closely mirrors our expectations thus confirming the HBT experiment and the existence of photons.

The purely classical picture does not describe the data in Table 2 as the coincidences between detectors A and B are very low, well within our accidental range. The α values for AG and BG are 127 and 175 respectively indicating correlation, while for AB $\alpha = 1$ which does not indicate correlation. If our light was simply being split in intensity, we should have a coincidence count between A and B that is equal to their individual counts. It appears that individual photons are being split at the beam splitter. The data also confirms the triple coincidence count between detectors A, B, and Gate (ABG) is very low, as expected.

In everyday interactions we cannot track individual photons and thus a stream of individual photons being sent down either path of the beam-splitter with a 50/50 probability leads

to the classical picture of light where the intensity of the light is simply split. In this particular set of data there is not a perfect 50/50 split between our detector A and Gate detector (AG) coincidences and detector B and Gate detector (BG) coincidences. This is reasonable because there are losses due to imperfections in the fiber optic cables, collimators, and the tip/tilt exactness of each detector.

4 Single Photon Interference

So far it has been shown that light is a particle phenomenon this picture sufficient in understanding light? In this experiment we will probe light's properties to determine why we need quantum mechanics at all.

Now that we have shown the existence of photons, we can show that these packets of light also behave like waves, highlighting the fundamental wave-particle duality. This is accomplished by showing individual photons interfering with themselves as they pass through a Mach-Zehnder interferometer (MZI). Detailed instructions for the alignment and setup procedure for the MZI can be found in Appendix C. The wave behavior of a single photon can be observed as a piezo-electric gently changes the path length of one of the arms of the MZI. As the path length changes, we can observe the count rate at the detectors and the coincidence count both decrease and increase, graphing these values allows us to examine the interference fringes. Interference fringes appear even as a result of just a single photon passing through our MZI.

4.1 Experimental Setup

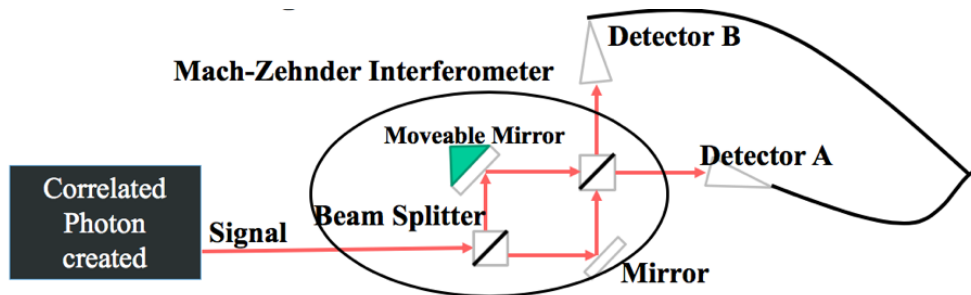


Figure 6: Schematic representation of the Single Photon Interference experiment

In order to adjust the path length of one arm, this MZI utilizes a piezo-electric as a spacer on a translational mount. This piezo-electric device physically expands when a voltage is applied to it. By regulating the voltage, one can very accurately adjust the positioning of our mirror and thus the path length of that arm of the MZI. Adjusting the path length of one arm by a single wavelength, 810nm, a complete interference pattern should be observed.

Note that our Gate detector is still setup to receive one of the photon pair, but is simply not included in Figure 6. The "Signal" drawn entering the MZI is one photon from the pair, while the other is sent to the Gate detector.

4.2 Explanatory visualization of Single Photon Interference

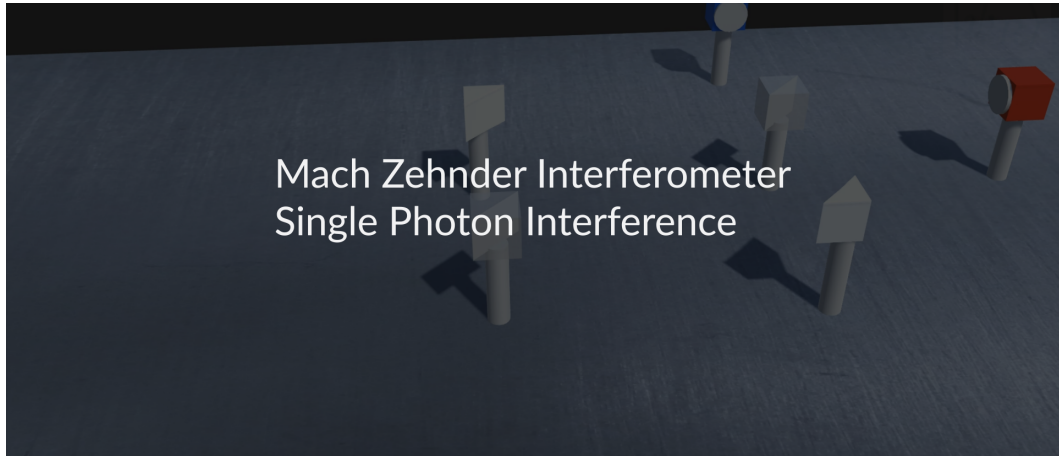


Figure 7: Link to a visualization of the Single Photon Interference experiment.
<https://youtu.be/mZjmwnaUC9o>

4.3 Single Detector Results

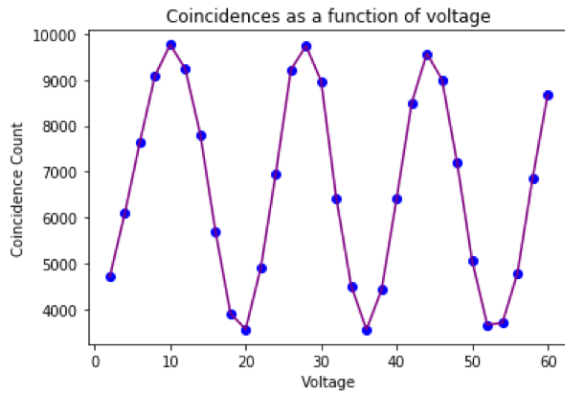


Figure 8: Data from detector A placed at the end of a single arm of the MZI. Coincidence Count is a rate of counts per 25s, Voltage in units of V.

Data for Figure 8 was collected every 2V increase in the piezo voltage. Data points are represented by blue dots, connecting lines are simply used to help visualize the pattern. Voltage represents a movement in the piezo-mounted mirror in the MZI, thus representing a change in the optical path length of one of the arms of the MZI. A change of 18V can be assumed to represent a change of 810nm because of the spacing of the interference pattern in Figure 8.

As the voltage over the piezo is varied, fluctuations in the number of coincidences between our detector located at one end path of the MZI and our Gate detector are observed. The clear pattern in Figure 8 is obtained by single photons behaving as waves and traveling down both arms of the MZI and interfering with each other at the second beam-splitter, but we are sending only a single photon through our system so how can a photon act as a wave?

Quantum mechanics describes light as a superposition of possible states. Light entering the MZI enters as a single input state and is subsequently split into two states when encountering the first beam-splitter [5].

$$|\psi_{input}\rangle = r|\psi_R\rangle + t|\psi_T\rangle \quad (4)$$

Here $r = |r|e^{i\phi_r}$ and $t = |t|e^{i\phi_t}$ represent the probabilities of entering the reflected and transmitted state respectively when the light is incident on the beam-splitter, note the complex phase factor $e^{i\phi}$.

Now one can consider the states after the initial beam-splitter, where $|\psi_A\rangle$ and $|\psi_B\rangle$ represent the output states of our MZI, either exiting on a path to detector A or B respectively. When light is incident on the second beam-splitter it is again split into two possible states so that the $|\psi_R\rangle$ and $|\psi_T\rangle$ states can be described along the orthogonal set of output states to represent the system as:

$$|\psi_R\rangle = r|\psi_A\rangle + t|\psi_B\rangle \quad (5)$$

$$|\psi_T\rangle = t|\psi_A\rangle + r|\psi_B\rangle \quad (6)$$

$$P_A = |\langle\psi_A|\psi_{input}\rangle|^2 \quad (7)$$

Equations (5)-(6) describe a decomposition of our two paths in the MZI onto our output states [2].

Equation (7) is the probability of an output state A (a photon hitting detector A). Since our beam-splitters have a $\frac{1}{2}$ chance of transmitting or reflecting the only difference in r and t arises from the phase difference imparted by unequal path lengths:

$$\delta_i = \frac{2\pi L_i}{\lambda} \quad (8)$$

$$\delta = \delta_R - \delta_T \quad (9)$$

Equation (8) describes the path length of each arm of the MZI, indexed by i . While Equation (9) represents the path-length difference of the entire system which is relevant for the probability difference between the two detector states.

This difference is only proportional to the path length L_i , since the wavelength λ is held constant [5]. So finally, the probability of detection is:

$$P_A = \frac{1}{2}(1 - \cos \delta) \quad (10)$$

$$P_B = \frac{1}{2}(1 + \cos \delta) \quad (11)$$

This probability changes as a function of the path length difference, thus we expect to see a pattern of coincidence counts as a function of the path difference: as can be seen in the interference pattern shown in Figure 8 [5]. This changing probability due path-length difference occurs with a single photon. Because of this superposition of states the single photon is interfering with itself at the second beam-splitter, thus explaining what we observe experimentally.

The exact distance the mirror moves as a function of voltage is unclear. A full cycle is expected every 810nm given Equation (8). The mounted angle of the MZI mirror is only roughly 45° and the piezo-electric used does not have a completely linear expansion as a function of voltage so finding an exact value of L_i is difficult. This information is insignificant however since one can derive that a change of 18V results in an effective change of 810nm

based on the placement of interference fringes in Figures 8 and 9.

4.4 Dual Detector Results

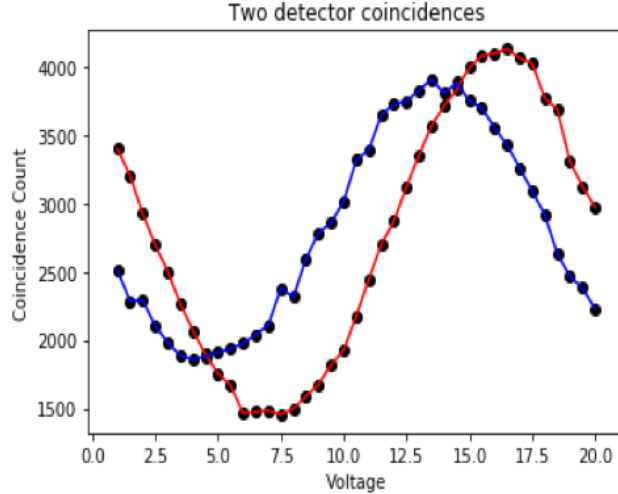


Figure 9: Data from both detectors of the MZI. Coincidence Count is a rate of counts per 15s, Voltage in units of V.

The red line in Figure 9 represents data points corresponding to coincidences between detector A and the Gate detector, while the blue line represents coincidences between detector B and the Gate. Detectors A and B are placed at the orthogonal output paths of the MZI, while the Gate detector is still kept outside of the MZI so that we can identify when the detectors are counting photons from the photon pair.

Examining each detector independently we observe the similar interference patterns; however, our orthogonal detectors should have a phase difference of 180° as can be seen from Equations (10)-(11). This is clearly not what is observed in Figure 9. This could be due to a problem with the particular experimental setup used in our lab and would require additional time to accurately diagnose. Going forward, it would be insightful to recreate this portion of the experiment to determine the source of this issue. This observation should not represent any systematic problem with the experimental setup itself, just with the particularity of our setup.

5 Possible Improvements and Extensions

A number of potential improvements to our setup have been identified. One improvement would be introduction of an automated system for data collection: especially in a classroom environment, an automated system would enable students to examine the effects of the experiment and check its validity without having to go through the tedious process of manual data entry from the simple Altegra VI program. Additionally, a step-by-step alignment process for these experiments, such as the one provided in Appendix C would've proven invaluable to quickly aligning the experiment. It is also imperative to systematically make sure each portion of the equipment is working before proceeding with any portion of the project: during the course of our experimental setup, we utilized a BBO crystal which had physical deformation caused by exposure to humidity. The BBO crystal is hygroscopic and should be kept in a closed environment with desiccant when not in use. Additionally, an exact measurement of piezo voltage to physical distance might be made, but this obviously varies for every piezo used. For a complete list of the equipment used please refer to Appendix A.

Rerunning the Single Photon Interference experiment might be of value so that there will be useful data for other lab setups to compare to.

The scope of quantum mechanical concepts that could be explored through this lab could be expanded fairly simply, first by utilizing the MZI in order to show Bell's inequality and Quantum Erasure by placing wave-plates along the arms of interferometer. This setup could also be adapted to examine the properties of optical gyroscopes by placing the setup on a rotating stage.

A Equipment

All the code used in this experimental setup can be found at:

<https://github.com/Fugos/Photon-Quantum-Mechanics-Data-Analysis>

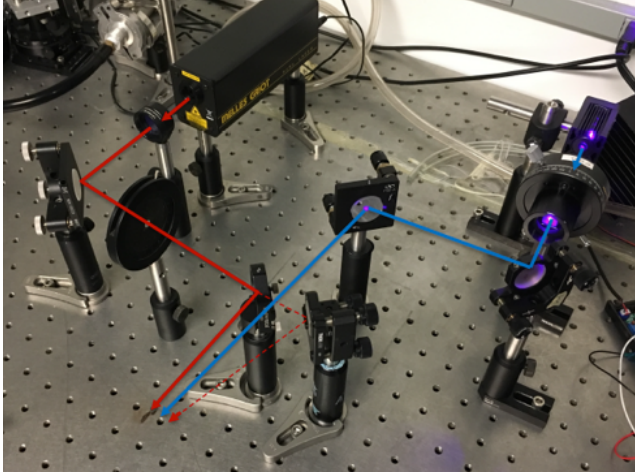


Figure 10: The HeNe and Blue laser setup is pictured. With this setup it is possible for our HeNe beam, the top-right black box laser, to go through a lens and eventually through the BBO crystal. A flipper mirror is placed so that when it is down the HeNe travels at 0° with respect to the crystal. When the flipper mirror is up the HeNe beam exits at 6° . The blue 405nm laser goes through a linear polarizer and is reflected so that it is along the 3° .

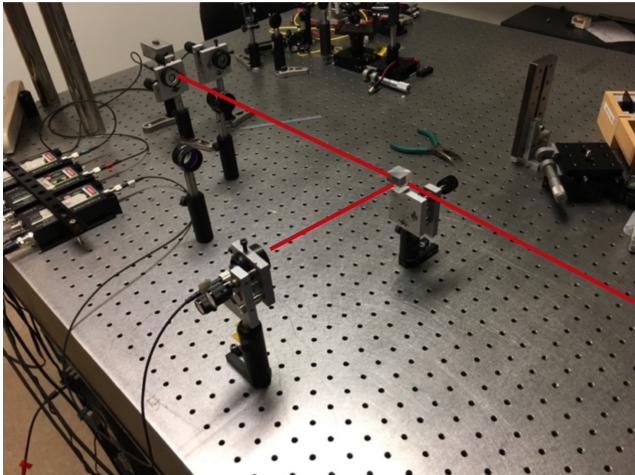


Figure 11: In this image is pictured the beam-splitter and the 3 detectors needed to conduct the experiment and their appropriate positioning relative to each other. The stream of correlated photons enters the beam-splitter from the left and half of the photons enter detector A, and the other half enter detector B. The gate detector is also pictured in the back right.

We used a variety of off-the-shelf optics equipment from Thor-Labs, Edmund Optics, and Newport Optics. Additionally, a number of parts were custom machined before we arrived, whilst some others we machined ourselves to match the specifications we needed.

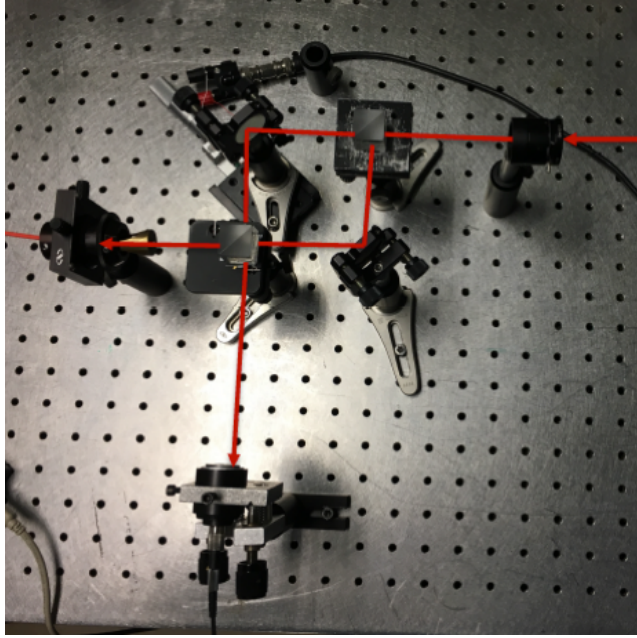


Figure 12: Pictured is our Mach-Zehnder-Interferometer with a spectrometer at one end and detector A at the other end. Also pictured is the piezo-electric's connection to the voltage controller and the iris placed before the MZI used for aperturing the HeNe beam for alignment.

The most important components are the BBO crystal which are just purchased from a number of different suppliers, the single photon counting modules from Excelitas (SPCM-EDU CD3375), and a collimator stack which we machined.

Figures 10, 11, and 12 picture how this equipment was utilized to create the schematics previously shown in figures 2, 4, and 6. Not pictured is the detector setup for the down-conversion experiment; however, it looks identical to Figure 11 just without the beam-splitter in place.

Note, the collimator has been referred to as the detector up until this point. This isn't exactly correct as the collimators are used to capture the light and transmit it to the single photon detector proper. The collimator consists of the collimator focusing lens, fiber optic, custom machined stand, custom machined filter holder, and a 810nm light filter.

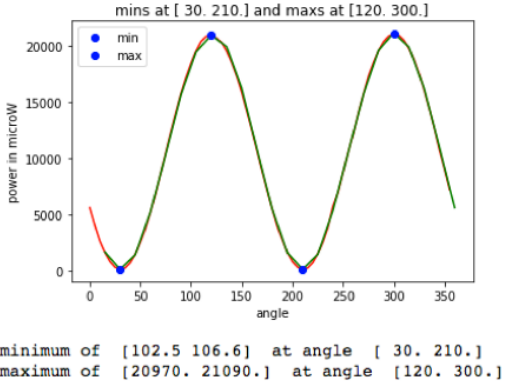


Figure 13: The BBO crystal is cut in a way that allows for horizontally polarized light to generate horizontally polarized entangled pairs. Measuring the power output of our laser as a function of the angle of a polarizing filter placed in front of it we found that the laser we used was actually polarized at 30° to vertical and so we place a polarizing filter in front of the laser to reduce excess noise imparted to our system.

Figure 13 illustrates an interesting circumstance of dealing with cheap lasers. The laser used had a polarization angle at 30° to horizontal which was not listed anywhere. When dealing with cheap off-the-shelf parts such as this it is useful to test whether the outputs are as intended.

The BBO crystal must be handled with care as it is hygroscopic and will be damaged if left out in normal humidity. The first crystal which we used was 3mm thick and was left out before we arrived, the damage to the crystal took a while to deduce until we discovered the hygroscopic property of the crystals. Our second crystal was 1mm thick, which has reduced efficiency as compared to the original 3mm, but is stored in a humidity-controlled bag which when not in use which should allow it to have a much longer usable life-span. A damaged crystal can be used a placeholder while aligning however.

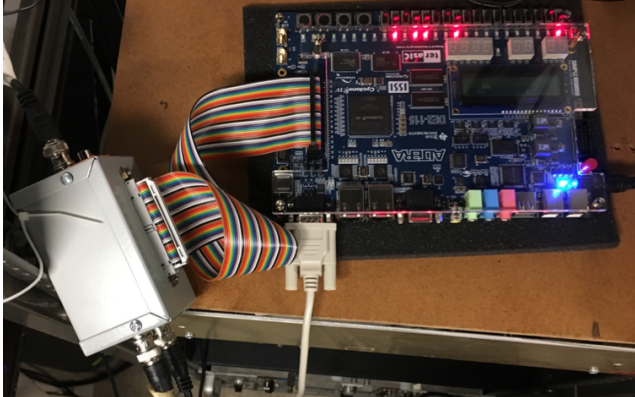


Figure 14: Pictured here is our converter-box: it features 4 BNC inputs and outputs them to the FPGA through a ribbon-cable. The FPGA is also pictured with its RS232 output, the ribbon cable, and a power cable plugged in. The red LEDs are enabled through software to be lit if its corresponding switch is enabled.

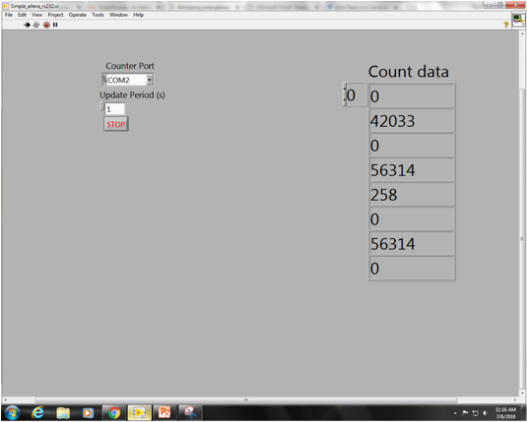


Figure 15: We obtain our data through a labview program written by Jesse Lord and M. Beck. We employ the simple Altegra labview VI which simply displays the number of counts for each detector and four configurable coincidence counts. The program simply takes a byte-stream from the FPGA and changes it to be human-readable.

In order to take the raw electrical pulses from our avalanche photo detectors, we employ a simple soldered circuit, our converter-box, and an Altegra DE2-115 FPGA with custom software, pictured in Figure 14. Our FPGA is acting as a CCU, Coincidence-Count-Unit, measuring the overlap between detector pulses. The simple software interface used in our setup is pictured in Figure 15. More complex labview programs exist for this purpose (available at <http://people.whitman.edu/~beckmk/QM/labview/labview.html>), including ones which utilize arduino driven piezos to automate data collection, but for our purposes this simplest labview program is sufficient.

The converter-box consists of 4 input BNC connections along the sides of an aluminum box that have a 50Ω resistor termination. These inputs are soldered to 4 wires on a ribbon-cable which is then crimped to a ribbon-cable input that is placed through the top of an aluminum case.

Our CCU software is primarily written by Jesse Lord of Whitman college; however, his VHDL program was written for an older DE2 board. A group at Berkley rewrote a portion of the program to allow it to function on the DE2-115, which we are using here. I made several alterations to the code as well, such as allowing the switch LEDs to light up and remapping which pins of the ribbon-cable represented which detector pulses (to make it compatible with our converter-box. The program takes the input pulses and produces a 1 clock-cycle delayed pulse (with a 50MHz clock, we are able to create a pulse that is 5×10^{-7} second time-delayed), using an XOR operation on these two pulses allows us to then create

a new pulse that retains its relevant timing information, but is much shorter (we are able to achieve around 8ns pulses of this kind from an original pulse from the detector of around 42ns). Simply applying an AND gate between the pulses (where the pulses have a voltage above 1V as these are analog pulses which trail off from a max of 2.2V to 0V) detects whether these pulses have arrived at the same time. The program also allows for us to adjust the amount of pulse-shortening by changing the amount of clock-cycles we wait, we control this using switches 16 and 17 on our FPGA board [1].

Which inputs are to have their coincidences measured between is also controlled by the FPGA switches: there are 4 possible coincidence count outputs, 4 switches control which inputs are used to achieve the coincidence count. For example, in the image below switches 1 and 3 are switched so the first coincidence count output is measuring the coincidences between B and B' inputs, while switches 4 and 7 produces a coincidence measurement between A and B' inputs for the second coincidence output.

Colgate university hosts a webpage with extensive information about this lab setup which may prove useful to those wishing to investigate this setup further http://departments.colgate.edu/physics/research/Photon/root/photon_quantum_mechanics.htm.

B Mach Zehnder Interferometer Alignment

The alignment of the MZI is not only interesting as part of the experimental setup, but the steps involved in its alignment highlight valuable quantum mechanical and optical properties.

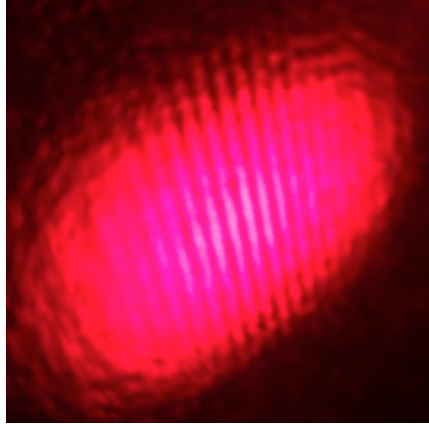


Figure 16: We first use our HeNe laser to adjust the MZI until it is displaying interference fringes in the HeNe beam itself, shown here. Once we obtain some interference we adjust the outputting beam-splitter until the interference fringes of the HeNe beam are so large that we see complete constructive or destructive interference of the beam and no individual fringes.

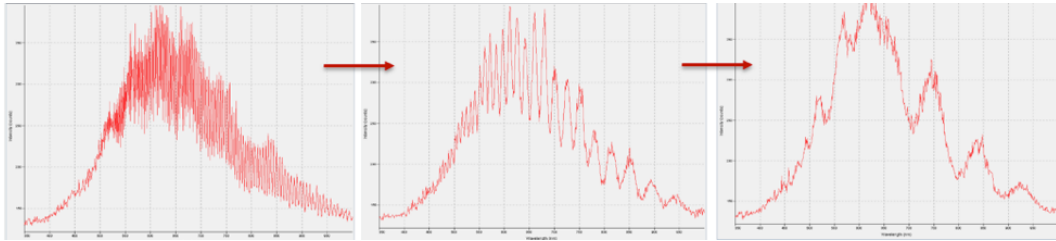


Figure 17: As we adjust the micrometer of our moveable mirror we see the white light interference pattern of our MZI changing. We want to adjust our MZI to produce interference fringes close to the coherence length of our down-converted light: we aim to increase the spacing between the fringes of white light as much as possible so that we can observe the greatest difference in coincidence counts.

The process involves using our HeNe alignment laser first as shown in Figure 16. Once the MZI is roughly aligned using this method we attempt to refine the path lengths between our two arms so that we witness white light interference. Using a simple white light point source, such as a bulb, along with a spectroscope mounted along an output path of the MZI. Figure 17 illustrates the process of subtly adjusting the MZI until white light fringes are an adequate width.

C Procedures

We have setup and conducted the parametric down conversion, Hanbury Brown-Twiss, and single photon interference experiments. Below is the best method for properly conducting each experiment that we formulated. There is some initial setup common to each experiment also detailed below.

C.1 Initial Setup

1. Mount the HeNe laser securely, the height of this piece will determine the height of everything else on the table.
2. Place a lens in front of the HeNe, this will enlarge it slightly which will be useful for aligning the collimators.
3. Put the BBO crystal in place and roughly place the collimators 1m away at 0° and 6° , with a beam dump at 3° .
4. Setup the mirrors for the HeNe so that we have a flipper going straight through the crystal to the collimator and another mirror going to our 6° collimator.
5. Align all lasers to be parallel to the holes on the table (except, obviously, the 6° mirror reflection).
6. Place the blue laser perpendicular to the ground (mounted with the white sticker not in the plane of the table) and a polarizer set to 0° in front of it.
7. Align the blue beam with mirrors so that it goes through the crystal and to the beam dump at 3° .
8. Tighten down all equipment on the side of the crystal with the lasers, you don't want to have it move at all.
9. Place collimators as accurately as possible at 0 and 6° 1 meter away from the crystal.
Beam dump at 3° .

C.2 Parametric Down Conversion

1. Remove the filters from the collimators.
2. Move the HeNe beams so that they now cover the collimators.
3. Adjust the Tip/Tilt of the collimators to achieve maximum output through the attached fiber optic. There is a tiny tip/tilt window in which the output is very bright.
This is critically important, without this step even if IR is hitting the collimator it will not be transmitted through the fiber optic.
4. Carefully place the filters back on the collimators without moving their tip/tilt rotations.
5. Start collecting data: turn the blue laser on, HeNe off, detectors on, FPGA on, labview on.
6. Adjust the TILT of the crystal until you find a peak in either detector's counts, refer to "The Dark Abyss" paper for troubleshooting this step [3]

C.3 Hanbury Brown-Twiss

1. Place a beam splitter in the path of the 0° collimator.
2. Place a 3rd collimator at 90° from the beam-splitter, the path length from the beam-splitter to each collimator should be roughly equal.
3. Remove the filters from the collimators and move the HeNe beam so that they now cover the collimators straight through.
4. Adjust the angle of the beam splitter so that the reflected HeNe beam covers the collimator.
5. Adjust the Tip/Tilt of the collimators to achieve maximum output through the attached fiber optic. There is a tiny tip/tilt window in which the output is very bright.
This is critically important, without this step even if IR is hitting the collimator it will not be transmitted through the fiber optic.

6. Carefully place the filters back on the collimators without moving their tip/tilt.
7. Start collecting data: turn the blue laser on, HeNe off, detectors on, FPGA on, labview on.
8. Adjust the TILT of the crystal until you find a peak in both detectors.
9. Adjust the tip/tilt of the non-flag collimators so that they maximize their coincidence counts with the flag, not their raw counts.

C.4 Single Photon Down Conversion

1. Place a beam splitter in the path of the 0° collimator, aligning the reflected portion of the beam with the holes of the table so that it is exactly at 90° .
2. Place an iris along the 0° path, making sure that it is not at an angle to the holes and that it is at the appropriate height. This allows us to aperture the HeNe beam so that it is even smaller thus allowing for more accurate alignment.
3. Place a mirror 4 inches from the beam-splitter, align the reflection so that it is at 90° using two irises
4. Place a mirror on a translation mount 4 inches from the beam-splitter, again aligning the reflection so that it is at 90° using two irises. Make sure that the translation stage is at 45° to the holes on the table.
5. Place the final beam-splitter exactly where the two beams cross. Align the angle of the beam-splitter so that the reflected beam is at the same angle as the non-reflect portion.
6. You should now see interference fringes in the recombined beam, use a diverging lens in order to better examine the fringes.
7. **Only** adjust the final beam-splitter until you see the fringes become larger than the beam itself, make sure the beams are still overlapping along both arms by removing the diverging lens.

8. Place a white-light point source such as a simple filament bulb before the first beam-splitter, along with a spectrometer along one of the arms of the interferometer (one can place the input along the path of the HeNe beam).
9. There should be interference fringes in the readout of the spectrometer now, adjust the micrometer of the moveable mount until the fringes are as large as the whole waveform.
10. Re-examine the HeNe beam fringes to make sure that they are not visible, if they are repeat steps 8-9. You may have to repeat these steps a few times.
11. Adjust the Tip/Tilt of the collimators to achieve maximum output through the attached fiber optic. There is a tiny tip/tilt window in which the output is very bright. **This is critically important**, without this step even if IR is hitting the collimator it will not be transmitted through the fiber optic.
12. Carefully place the filters back on the collimators without moving their tip/tilt.
13. Adjust the **tilt** of the crystal until you find a peak in both detectors.
14. Start collecting data: turn the blue laser on, HeNe off, detectors on, FPGA on, labview on.

References

- [1] D. Branning, S. Bhandari, and M. Beck. Low-cost coincidence-counting electronics for undergraduate quantum optics. *American Journal of Physics*, 77(7):667–670, 2009.
- [2] E. J. Galvez, Charles H. Holbrow, M. J. Pysher, J. W. Martin, N. Courtemanche, L. Heilig, and J. Spencer. Interference with correlated photons: Five quantum mechanics experiments for undergraduates. *American Journal of Physics*, 73(2):127–140, 2005.
- [3] Kiko Galvez. In the Dark Abyss: No Coincidences. What to Do?, 2015.
- [4] George Marcus. Colloquium, June 2017.
- [5] Brett J. Pearson and David P. Jackson. A Hands-on Introduction to Single Photons and Quantum Mechanics for Undergraduates. *American Journal of Physics*, 78(5):471–484, February 2010.